Taiwania, **46**(3): 246-273, 2001

The Effect of 4-Methylmorpholine N-oxide Monohydrate (MMNO·H_2O) on Pollen and Spore Exines

John R. Rowley[1, 5], Nina I. Gabarayeva[2], John J. Skvarla[3] and Gamal El-Ghazaly[4]

(Manuscript received 2 August, 2001; accepted 6 September, 2001)

ABSTRACT: Mature pollen grains of *Betula pendula*, *Borago officinalis*, *Calluna vulgaris*, *Fagus sylvatica*, *Lilium longiflorum*, *Pinus sylvestris* and spores of *Lycopodium clavatum* were exposed to 4-Methlymorpholine N-oxide monohydrate (MMNO·H_2O) at 80°C for times varying from 30 minutes to 310 minutes. After 30 minutes microchannnels had expanded from approximately 25 nm to 50 nm in diameter, the channel size during development is approximately 50 nm. After about 5 hours in MMNO·H_2O pronounced changes in exine morphology were observed except in *Calluna*. Changes in exine morphology of *Borago* and *Pinus* involved sporopollenin that our previous studies indicated had been added late in development. Early in development sporopollenin accumulates on Sporopollenin Acceptor Particles (SAPs) that are part of the plasma membrane surface coating (tufts, the unit-structures of exines). Subsequently, late in development, secondary sporopollenin is added between tufts or on their surfaces. At this stage SAP cross linkages permeate the exine. Our interpretation is that MMNO·H_2O, as a potent solvent for polysaccharide, penetrates the exine through the core zone (microchannels) of tufts and tuft cross linkages. When polysaccharide is removed exposure to water and solvents normally used for TEM preparation cause fracture of exine components. Exine changes during MMNO·H_2O in *Betula* and *Fagus* may be similarly interpreted since erosion parallels the orientation of the tuft core and its subunits. In *Lilium* the most slender columellae consisting apparently of one tuft were eroded enough to expose coils of outer (binder) zone. In *Lycopodium* the MMNO·H_2O resulted in exposure of closely spaced (approximately 10nm) circumferentially oriented lamellae that are grouped into linear structures. These linear structures are circular in cross section and greatly variable in size (most are 100–200 nm in diameter). Scans using atomic force- and scanning tunnelling- microscopy suggest that the mainly longitudinal subunits appear to be helical, and radial cross linkages between the structures can also be discerned. No change, other than enlargement of microchannels, could be seen in the endexines of the species studied. Our interpretation is that the greater resistance of the endexine than the ectexine is due to close packing of tufts without any secondary deposition of sporopollenin.

KEY WORDS: **AFM, *Betula*, *Borago*, *Calluna*, Ectexine, Endexine, *Fagus*, *Lilium*, *Lopezia*, *Lycopodium*, Microchannels, MMNO·H_2O, *Pinus*, Secondarily Accumulated Sporopollenin, SAPS, STM, *Triticum*, Tuft.**

INTRODUCTION

Initially, 4-Methylmorpholine N-oxide monohydrate (MMNO·H_2O) was used in the study of pollen grains to free the exine from attachment to the polysaccharide-rich intine in an effort

1. Botany Department, Stockholm University, SE-106 91 Stockholm, Sweden.
2. Komarov Botanical Institute, Popov st. 2, St. Petersburg, 197376, Russia.
3. Oklahoma Biological Survey and Department of Botany-Microbiology, University of Oklahoma, Norman, OK 73019-6131, USA.
4. Gamal El-Ghazaly, our dear friend and collaborator, died on 13 January 2001. We will miss him very much.
5. Corresponding author.

to obtain isolated living protoplasts (Loewus *et al.*, 1985; Baldi *et al.*, 1987; Tarlyn *et al.*, 1993). Unaccountably, MMNO·H_2O exposure at temperatures near its melting point (about 80℃) resulted in some destruction of exines. The method resulted in isolated exines of *Lilium longiflorum* for analysis of their sporopollenin content using ^{13}CNMR spectroscopy (Espelie *et al.*, 1989).

Descriptions of exine structure in this report make use of exine units that Rowley and Dahl (1982) called "tufts". The tuft model (Rowley, 1987) has received support from the analyses of Thom *et al.* (1998) using TEM, SEM and the X-ray microscope on reaggregated materials obtained after fractionation of dissolved sporopollenin. The minimal size for a tuft is about 70 nm outside diameter with a core zone about 40 nm in diameter. Claugher and Rowley (1990) illustrate "tufts" in the exine of *Fagus sylvatica* ranging in diameter from70 up to 250 nm; with some tufts having distal tips that necked down to only 70 to 100 nm in diameter.

Our aim was to study the ultrastructural aspects of the dissolution of the exine reported by Loewus *et al.* (1985) and Espelie *et al.* (1989). We wished to find out which portions of the exine were extracted or eroded by exposure to MMNO·H_2O. We wished also to see what the effect of MMNO·H_2O extraction was upon histochemical tests for the intine and endexine and ectexine of the exine.

MATERIALS AND METHODS

Dry pollen grains of *Lilium longiflorum* Thunb., *Betula pendula* Roth., *Calluna vulgaris* (L.) Hull., *Fagus sylvatica* L., *Borago officinalis* L., *Pinus sylvestris* L., and spores of *Lycopodium clavatum* L. were added to MMNO·H_2O melted at 80℃. Aliquots were intermittently sampled for 310 minutes when many exines showed pink-red metachromasia in Toluidine blue, indicating exposure of polysaccharides (see discussion). After washing the mixture of the above seven species free of MMNO·H_2O, the grains were well mixed and divided. Half were prepared for embedding in epoxy resin with or without secondary fixation/staining by osmium tetroxide (Os).

The pollen was washed in 70% acetone, dried in 100% acetone and embedded in Araldite-Epon epoxy resin (Mollenhauer, 1964). Thin sections were stained for TEM with a saturated solution of uranyl acetate in ethanol and 0.2% lead citrate (pH 12.2), unless otherwise noted in the illustration descriptions. The sections were examined with Hitachi H-600 and Zeiss EM-10A transmissions electron microscopes.

For scanning microscopy (SEM) fresh pollen was acetolyzed (Erdtman, 1960), washed, dried and mounted on an SEM stub and coated with gold/palladium (60/40). A Hitachi S800 field emission scanning electron microscope was used for observation.

For atomic force microscopy (AFM) and scanning tunnelling microscopy (STM) methods for specimen preparation and instrumentation used are detailed in Wittborn *et al.* (1996).

RESULTS

Betula pendula

In mature pollen of *Betula* fixed from living anthers the tectum is crossed by microchannels that are about 25 nm in diameter. Such channels are illustrated in cross and tangential section in Figures 1 and 2. In mature pollen the columellae are commonly

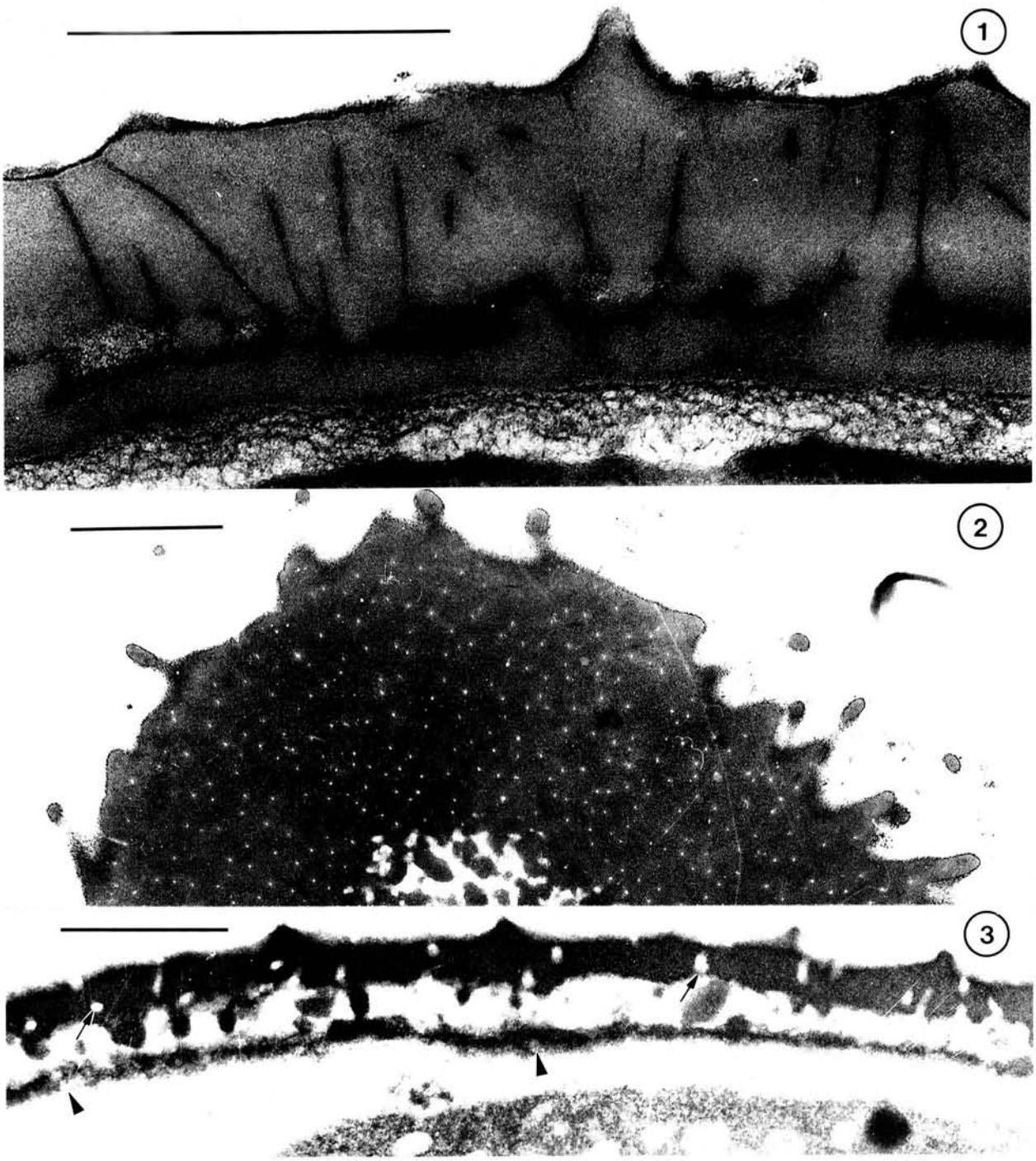

Figs. 1-3. TEMs of *Betula pendula* exines. Figs. 1, 2. Untreated exines illustrating channel diameter commonly seen after preparation for TEM. In both radial (Fig. 1) and transverse sections (Fig. 2) the channels are generally about 25 nm in diameter. Fig. 3. After exposure to $MMNO \cdot H_2O$ for 30 minutes channels (arrows) in the tectum are 40-50 nm in diameter; there are also faint outlines of channels (arrowheads) of similar size in the foot layer. Bars: 1 μm.

compressed between tectum and foot layer in what Dunbar and Rowley (1984) referred to as a "lazy-Z" configuration. The columellae are so compressed, that based on thin sections, they may appear to be granular.

Following exposure to MMNO·H_2O, microchannels in mature pollen were enlarged to about 50 nm in diameter (Figs. 3-8). This is the diameter of the core zone ("microchannels") of tufts during early development of the columellae (Dunbar and Rowley, 1984; El-Ghazaly and Jensen, 1985). The outside diameter of the binder zone of tufts in the tectum was variable although most were about 160 nm (Figs. 4, 6, 8). Columellae in cross (Figs. 5, 6) and longitudinal sections (Figs. 4, 7) range in diameter from 120-240 nm. Most columellae are upright and radially oriented after MMNO·H_2O exposure (Figs. 3-6), as they are during development. The diameter of the core zone in columellae also was extremely variable (from about 40 to 150 nm) in Figures 8, and 9. The binder zone of tufts in the tectum and in columellae appears solid and is highly contrastable whereas the "secondarily accumulated" exine between the tufts, in the tectum, is greatly eroded (Fig. 6). Spinules are about 150 nm in diameter, about the size of tuft units in the tectum. Most spinules in these figures are sectioned obliquely. The spinule (S) in Figure 6 shows the broad and tapering base common to *Betula*. The endexine is thin (20-30 nm thick) except under apertures where it has many "lamellae" (Fig. 7). For TEMs of untreated pollen of *Betula* in several stages of development see El-Ghazaly and Grafstrom (1995).

Borago officinalis

The gemmae on the tectum of the exine on mature pollen of *Borago* have a striate structure (Ben Saad-Liman and Nabli, 1984; Rowley *et al.*, 1999b). After the tetrad stage there are small (10-15 nm in diameter), spherical structures at the distal position of columellae (Fig. 12). These structures that we have called "Sporopollenin Accepter Particles" (SAPs; Rowley *et al.*, 1999b) were traceable in progressive stages of exine development to formation of the gemmae during development (Fig. 12). There is no indication in the gemmae of mature pollen (Fig. 13) of these small discrete spheres (SAPs).

After MMNO·H_2O exposure the supratectal gemmae of mature pollen lose their striate coating of sporopollenin and become structurally like they were early in development (Figs. 10, 11). In addition these "early structures" show a positive reaction to cytochemical reactions for protein (Fig. 10) and for lipids and/or protein (Fig. 11).

Calluna vulgaris

The exine of *Calluna* is very resistant to erosion under several conditions. Its high resistance to degradation in sediments was shown by pollen analytical studies in northern Europe where *Calluna* pollen contributed 90% or more of the recorded non-arboreal pollen (Erdtman, 1943; Faegri and Van Der Pilj, 1966; Faegri and Iversen, 1989; Moore *et al.*, 1991).

The ectexine as well as the endexine of *Calluna* pollen appears undamaged following MMNO·H_2O exposure. In the control section the channels are about 25 nm in diameter (Fig. 14). Microchannels were enlarged by MMNO·H_2O to 40-50 nm in diameter (Figs. 15, 16). The tuft-units remained in hexagonal close-packed raspberry-like arrangement illustrated by Hesse (1985) and Dahl and Rowley (1991: Fig. 53) through exposure to either MMNO·H_2O or potassium permanganate.

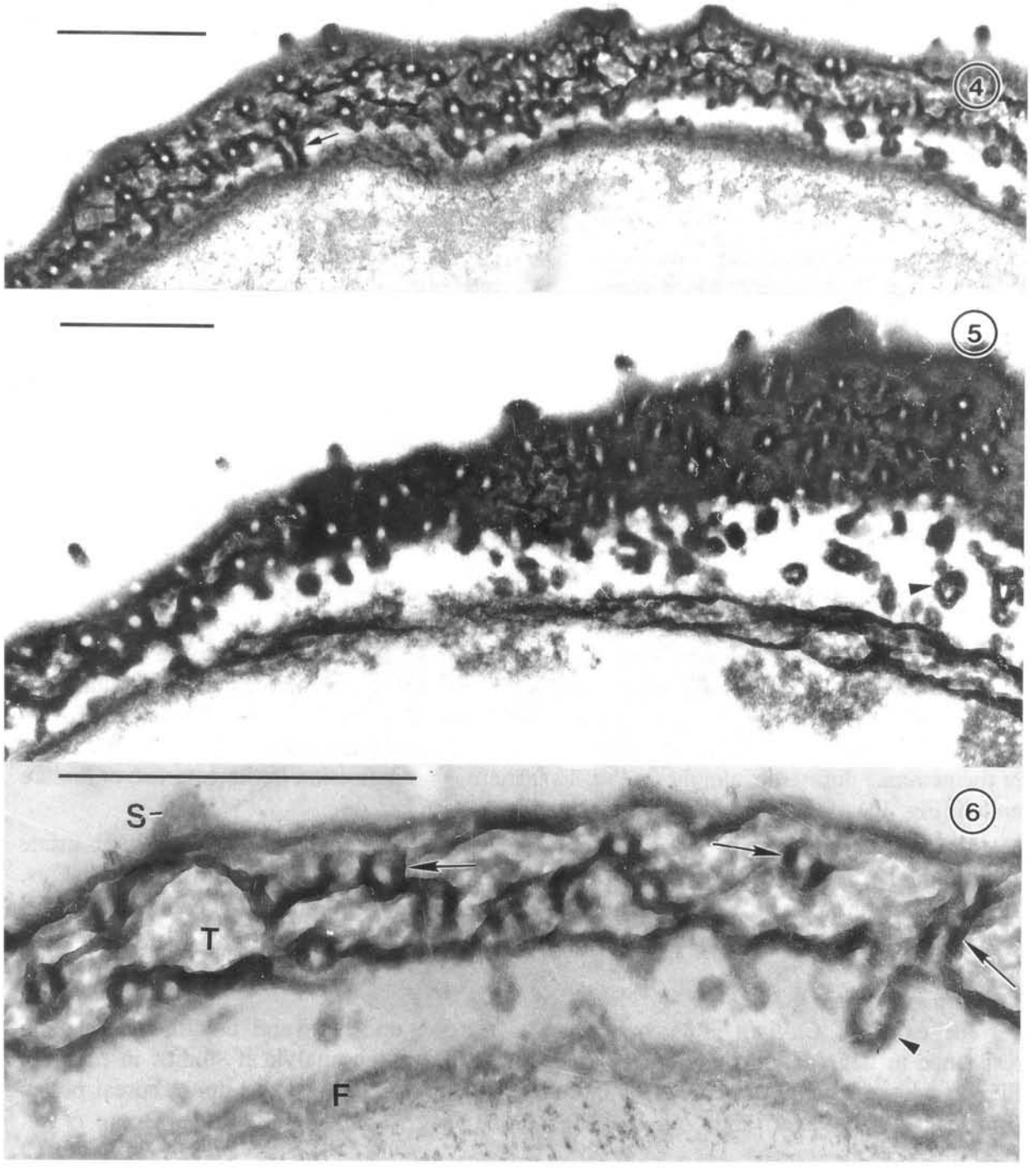

Figs. 4-6. TEMs of *Betula pendula* exines exposed to MMNO·H_2O for 310 minutes. Figs. 4, 5. Each tuft shows a low contrasted core (about 50 nm diameter) with a darkly contrasted binder zone (about 160 nm diameter). Columellae have a dark binder in cross (arrowhead) and longitudinal (arrow) sections. Spinules, columellae and tufts (in the tectum) are about 160 nm in the diameter. Fig. 6. The distal portions of spinules (S) sectioned medially have a diameter similar to that of the binder zone (arrows) of tufts in the tectum. The parts of the tectum (T) and foot layer (F) having intermediate contrast may consist of secondarily deposited sporopollenin. Columellae in oblique section (arrowhead). Bars: 1 μm.

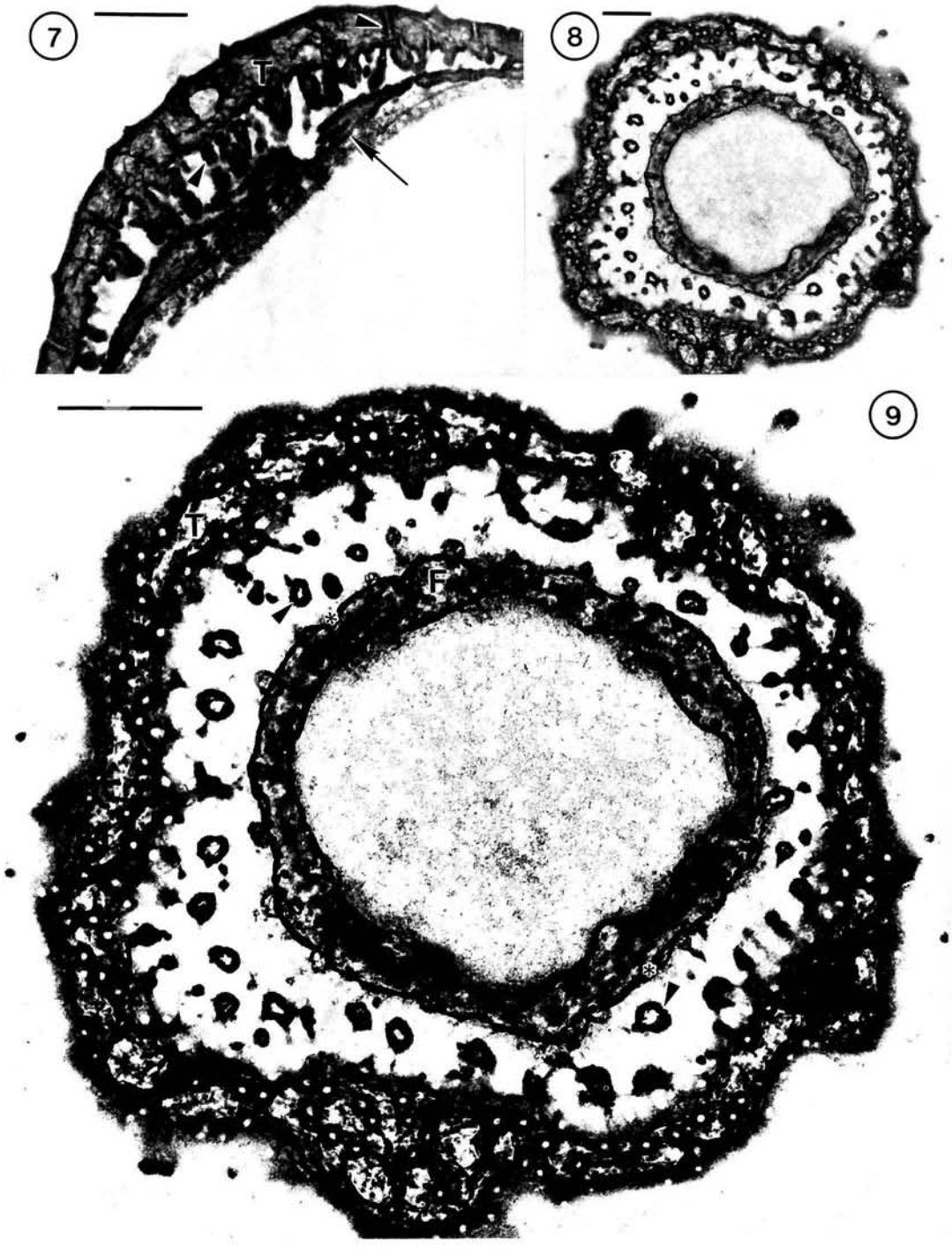

Figs. 7-9. TEMs of *Betula pendula* exines exposed to MMNO·H_2O for 310 minutes. Fig. 7. The apertural regions have several endexine "lamellations" (arrow) while elsewhere the endexine is very thin (about 10-15 nm). These endexine lamellations show the same high contrast as does the binder zone of tufts (arrowheads) in the tectum (T) and columellae. Figs. 8, 9. The light print in Fig. 8 emphasizes the difference between the dark tuft binders in the tectum and secondarily accumulated sporopollenin between them. It also shows the poor order of the dark binder components in the foot layer. Fig. 9 shows that the spinules are darkly contrasted like the tuft binders in the tectum (T) and columellae (arrowheads). The darkly contrasted boundary at the inner side of the foot layer (F) is the endexine. The continuous dark layer at the outer side (asterisk) of the foot layer is not explained by our interpretations. Bars: 1 μm.

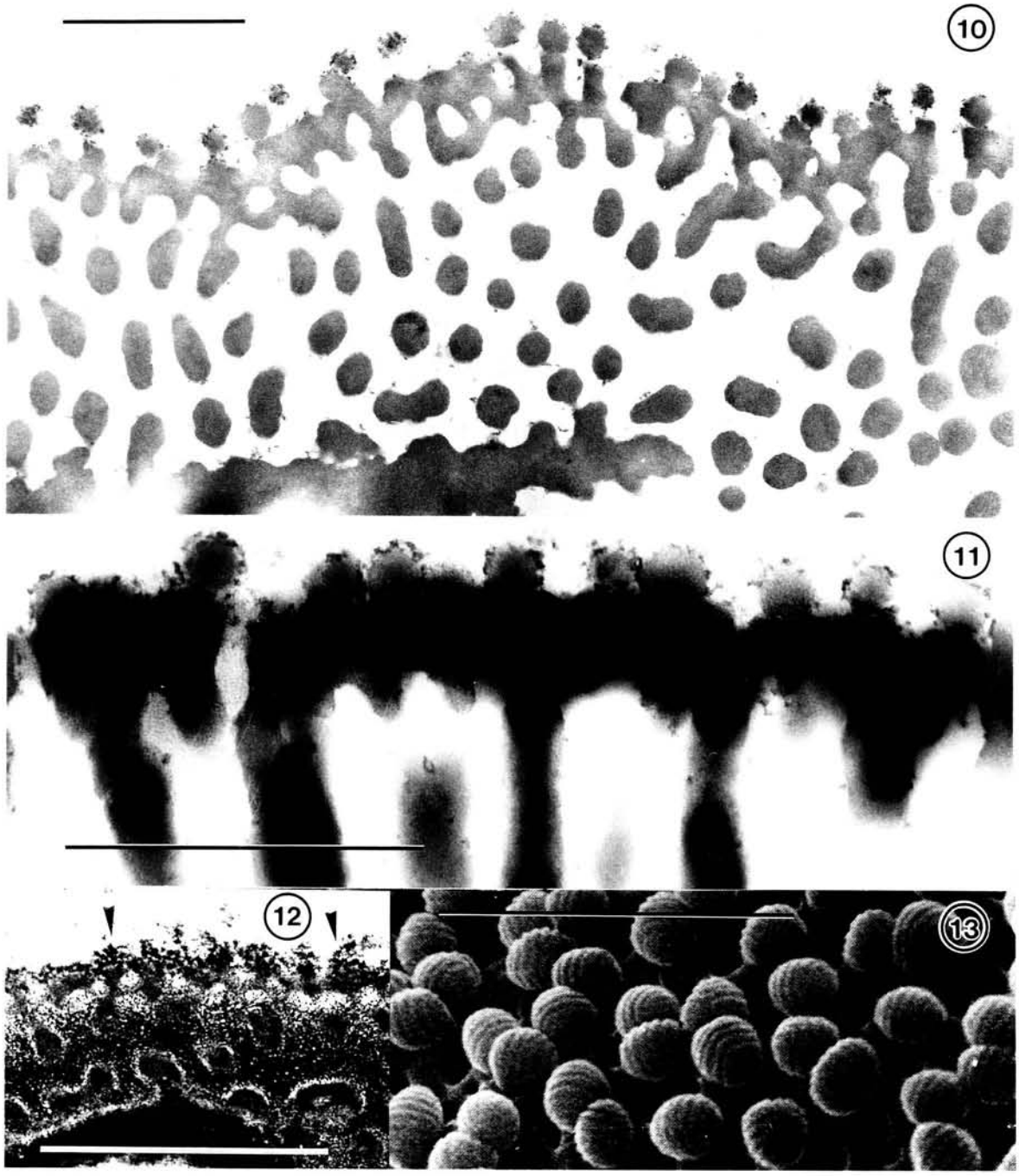

Figs. 10-13.TEMs of *Borago officinalis* exines. Figs. 10, 11. Exines exposed to $MMNO \cdot H_2O$ for 310 minutes. The outer apparently secondarily accumulated sporopollenin (seen in the surface of Fig. 13) is entirely eroded. The gemmae of the exine are as they were during early development. The cytochemical test, PTA in 10% in acetone, a general protein stain (Pease, 1968), is positive for the SAPs on these gemmae. Fig. 11. This material was exposed to OsO_4 before embedding for TEM. There was no other section stain, osmium binds to proteins as well as lipids. Fig. 12. A stage early in development of the gemmae. Fig. 13. SEM of mature pollen. In mature pollen the SAPs are enveloped by ridges of secondarily accumulated sporopollenin. Bars: 1 μm.

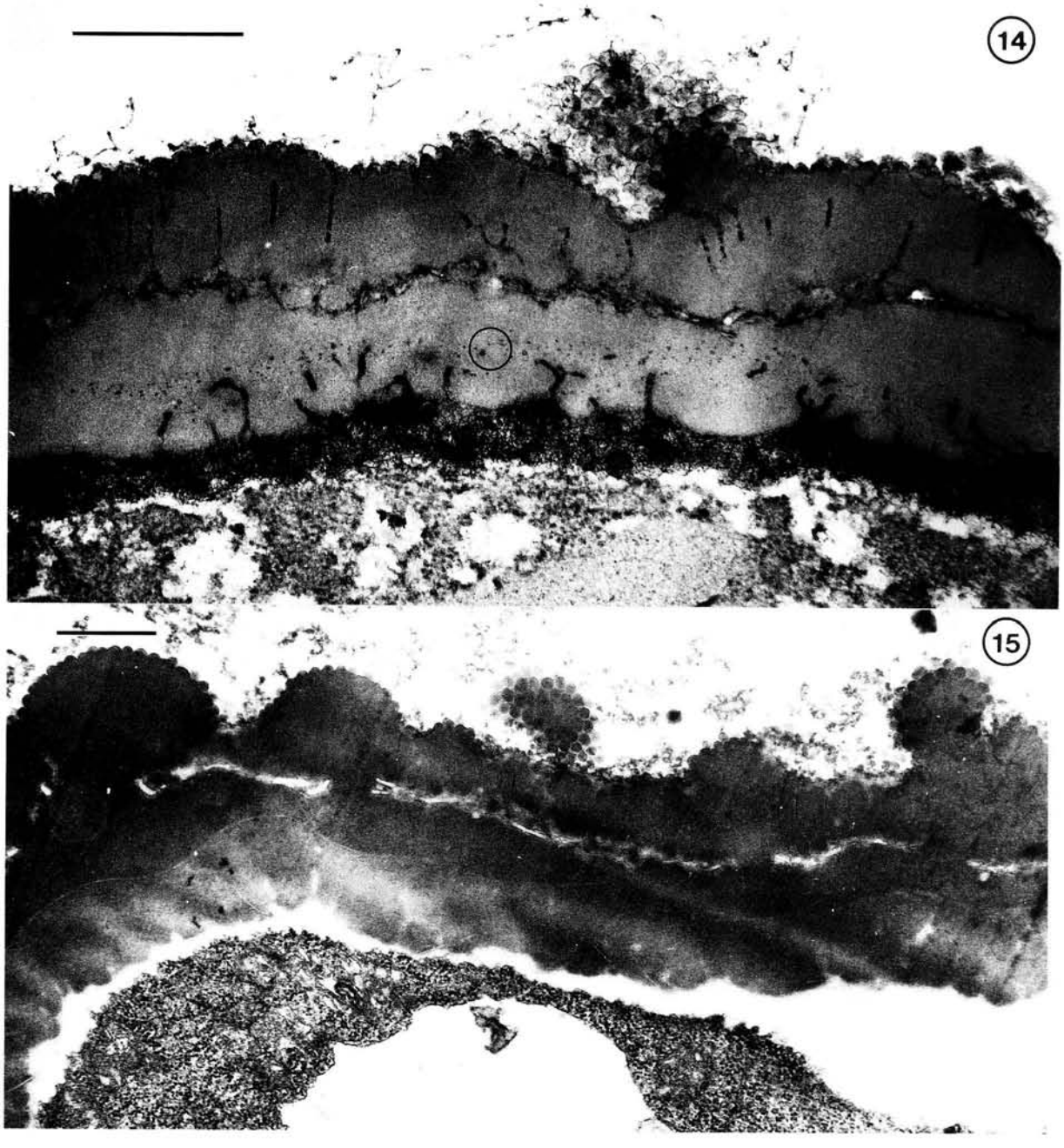

Figs. 14-15. TEM of *Calluna vulgaris* exines. Fig. 14. Untreated exine. The hemispheroidal distal ends of the exine tufts are prominent. Microchannels are about 25 nm in diameter. No microchannels are evident in the foot layer. The intine is prominent. The osmium-UA-Pb staining strongly contrast material in MMNO·H_2O channels and intine. The ectexine and endexine are contrasted the same. A zone of small dark spots (circle) shows the region between foot layer and endexine. Bar: 1 μm. Fig. 15. After 310 minutes exposure to MMNO·H_2O. The exine is not noticeably different from the untreated exine in Fig. 14 except for channels in the exine that are 40-50 nm in diameter and a slight contrast difference between ectexine and endexine. The intine has been removed by MMNO·H_2O. Bars: 0.50 μm.

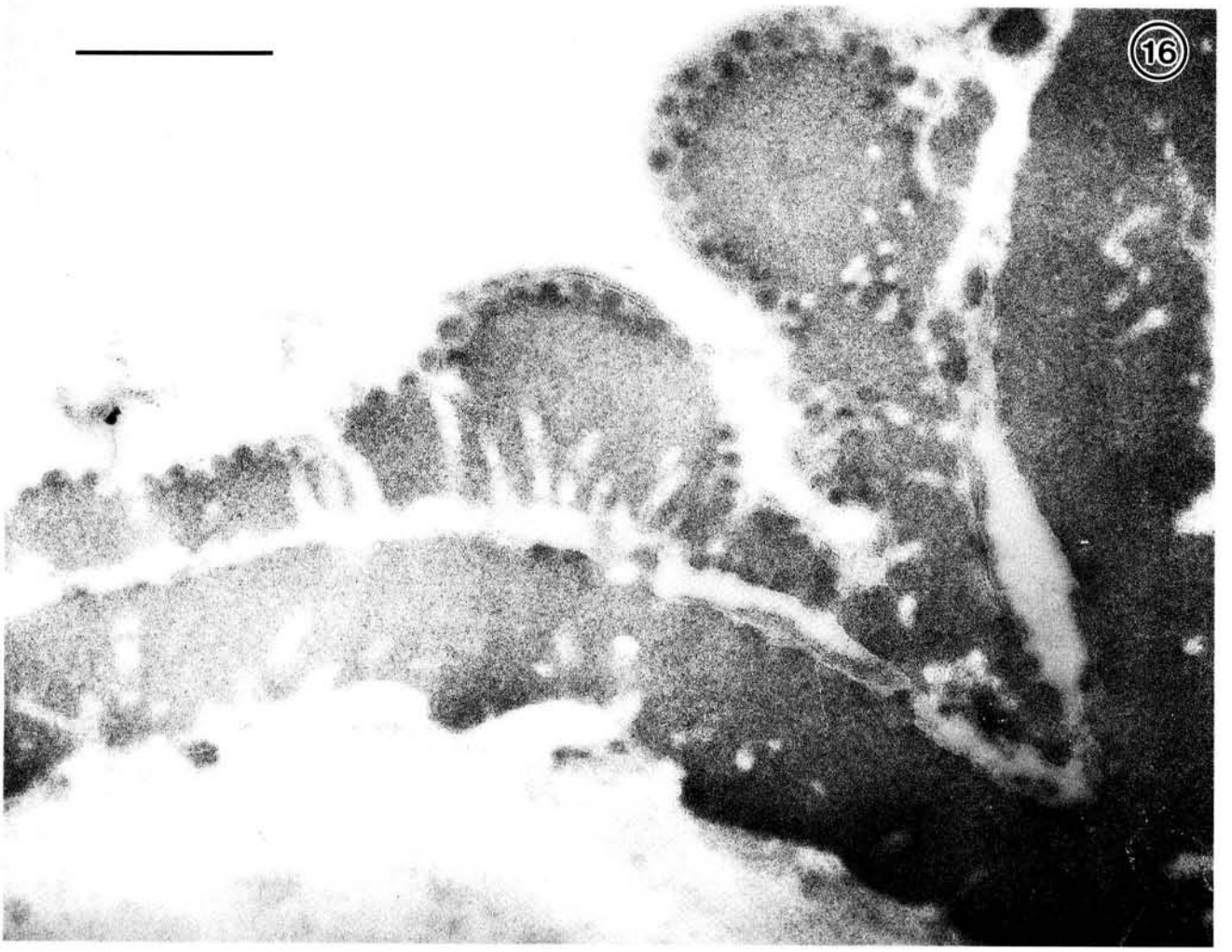

Fig. 16. TEM of portions of *Calluna vulgaris* exines in a permanent tetrad exposed to MMNO·H_2O for 310 minutes. The distal ends of the tufts are seen in a surface arrangement of nested (close packed) hemispheres or circles, depending on section plane. The microchannels were enlarged in both ectexine and endexine to 40-50 nm from the about 25 nm size in Fig. 14. Bar: 0.5 μm.

The explanation suggested by Rowley (2001) for the equal or, at least, similar resistance to erosion of the two exine zones is that the ectexine of *Calluna*, like the endexine, has very little or no secondarily accumulated sporopollenin between tufts.

Fagus sylvatica

In the mature exine of *Fagus* many of the tufts making up the tectum were circumferential in orientation, while in columellae the tufts were radial (Claugher and Rowley, 1990). Claugher and Rowley (1990) found that tufts were 70-100 nm in diameter in young stages but commonly became 200-250 nm wide in mature exines. The distal ends of some of these large tufts necked down in size to about 100 nm at distances of 0.5 μm or more from their outer tip (Claugher and Rowley, 1990: Fig. 14). Most of these features are apparent in Figures 17-19.

After exposure to MMNO·H_2O the endexine was much less eroded in all taxa. In the lower exine in Figure 24 the ectexine is greatly disrupted but the endexine appears to be little affected.

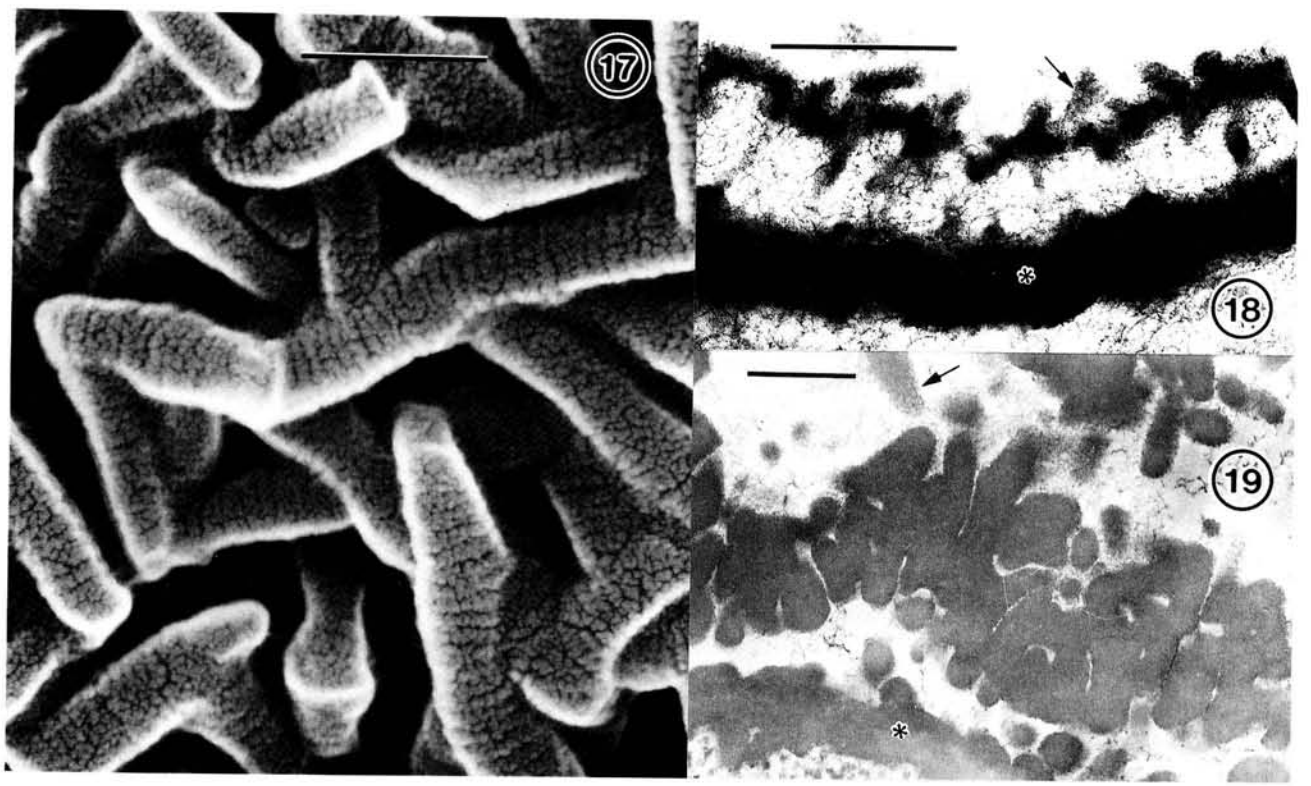

Figs. 17-19. SEM (Fig. 17) and TEMs (Figs, 18, 19) of *Fagus sylvatica* exines. Control samples. Fig. 17. An SEM of mature acetolyzed pollen. The processes (tufts) that make up the exine range in width from 100 to about 300 nm at the surface of mature pollen. The surface structure evident in the micrograph appears to be a coiled-coil. Bar: 0.5 μm. Figs. 18, 19. Somewhat oblique sections of a late microspore stage (Fig. 18) and mature pollen (Fig. 19). Fine surface structure (arrows) may be seen in both figures. An asterisk marks the foot layer and endexine. Bars: 0.5 μm.

All pollen grains exposed to MMNO·H_2O for 310 minutes were mixed throughout that period. There was variation in exine erosion in all species but various levels of erosion were seen with special prominence in the exines of *Fagus*. Three greatly different levels of exine erosion were apparent in the three adjacent grains in Figure 28. The most severely eroded exine (Fig. 24) is adjacent to one that is little changed from the untreated control (Fig. 19). There are some wide channels (50 nm or more) in the endexine, most frequently in apertural regions (e.g., Figs. 20, 22) and near apertures. The endexine is little affected by the exposure to MMNO·H_2O (Figs. 20-28). The same procedure caused extensive erosion to the ectexine (e.g., Figs. 22-24).

The PTA-in 10% chromic acid reaction for polysaccharides shows that MMNO·H_2O removed polysaccharides in the region of the intine and cytoplasm (Figs. 25, 26). The pollen in Figures 27 and 28 was reacted with PTA in 10% acetone, which is considered to contrastproteins. The intines are contrasted (Figs. 27, 28) in spite of the MMNO·H_2O extraction of carbohydrates, due to protein in association with intines. Starch has been extracted by MMNO·H_2O from plastids (Fig. 27) but the protein around former starch grains in plastids is contrasted.

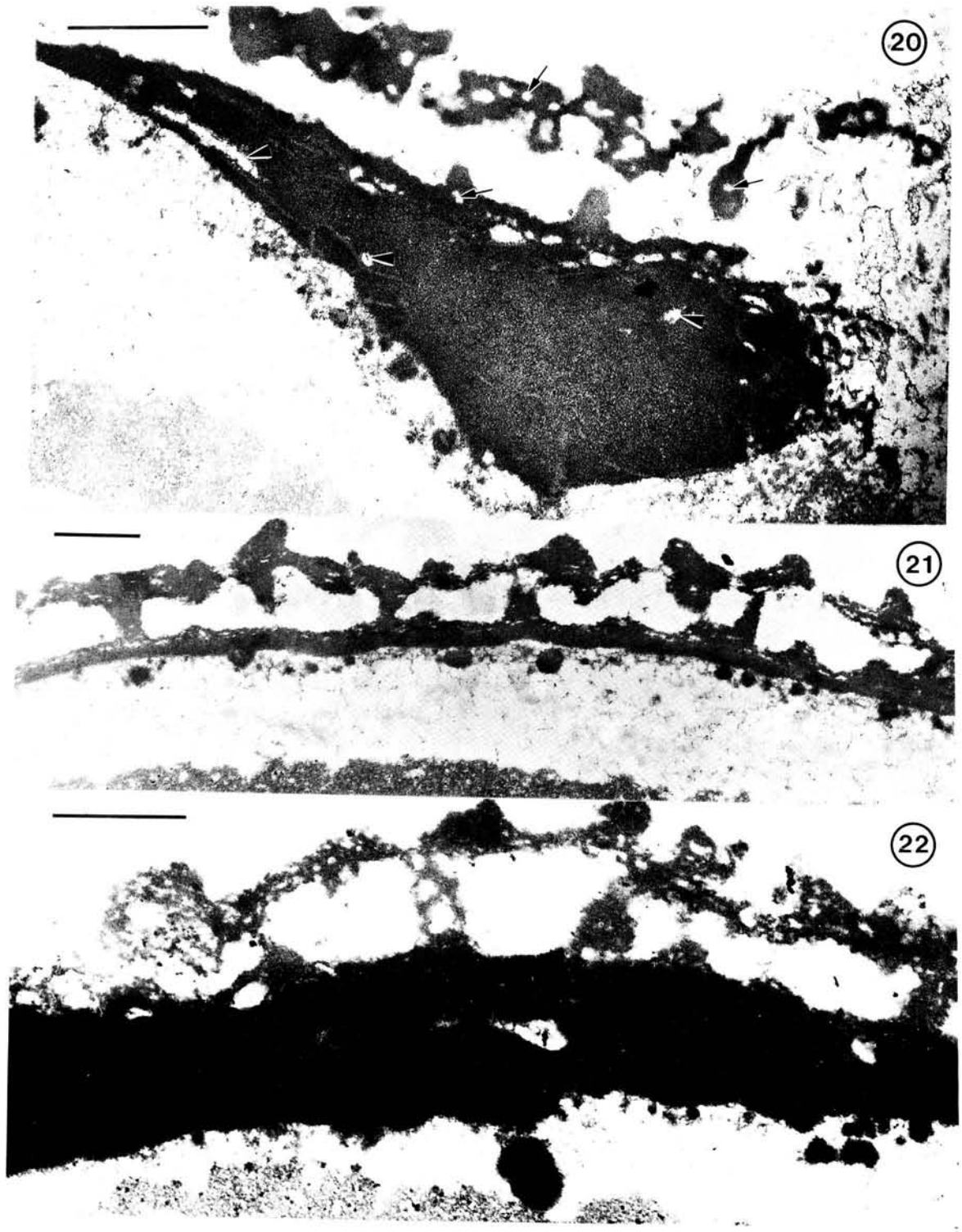

Figs. 20-22. TEMs of *Fagus sylvatica* exines exposed to MMNO·H_2O. Fig. 20. Exposure for 30 minutes. The core zone of the tufts ("microchannels") in both the ectexine (arrows in tectum, columellae and foot layer) and endexine (arrowheads) are low in contrast. The endexine is thicker toward the aperture to the right. Bar: 0.5 μm. Figs. 21, 22. Exposed for 310 minutes. The tectum and foot layer are eroded, especially in Fig. 22. The endexine in Fig. 22 is darkly contrasted except for a few low dense core zones. Bars: 0.5 μm.

Figs. 23-26. TEMs of *Fagus sylvatica* exines exposed to MMNO·H_2O for 310 minutes. Fig. 23. There are tuft core zones in cross section (arrows) and cores in radial arrangements in columellae (arrowheads). Low contrast sites in the tectum are oriented in a variety of directions as they are also in the tectal processes (cf. Fig. 17). The endexine (asterisk) seems to be without erosion. Fig. 24. Phosphotungstic acid (1%) in 10% chromic acid intensely contrasts acidic polysaccharides (Pease, 1968). The ectexine tectum, columellae and foot layer are very greatly eroded in the lower exine while the endexine (asterisk) remains intact. The upper exine could almost serve as an untreated control. Only one low contrast core zone (arrow) is apparent. Figs. 25 and 26. The section was reacted with 1% phosphotungstic acid in 10% chromic acid to contrast acid polysaccharides. Figs. 25 and 26 are from the same negative and show that there is little contrast in the intine region (asterisks), cytoplasmic surface or in the cytoplasm. Bars: 1 μm.

Figs. 27, 28. TEMs of *Fagus sylvatica* exines exposed to MMNO·H_2O for 310 minutes. Figs. 27, 28 were contrasted by phosphotungstic acid in 10% acetone, a general protein stain (Pease, 1968). Fig. 27. The contrast in the intine (star) is presumed to be due to protein. In plastids the starch was removed by MMNO·H_2O but protein around the starch grains (s) is contrasted. The ectexine (arrow) is greatly eroded but not the endexine (asterisk). Fig. 28. These exines show three different degrees of erosion. Bars: 1 μm.

Figs. 29-31. TEMs of *Lilium longiflorum* exines. Figs. 29, 30. Exines exposed to MMNO·H_2O for 310 minutes. Fig. 31. Exine was exposed to acetolysis followed by potassium permanganate. Fig. 29. The massive muri are eroded centrally and the slender columellae exposed in some planes of section are eroded enough to reveal the coiled substructure of the columellae. Fig. 30. The columella shows a coiled structure. The micrograph is from a section serial with the one in Fig. 29. Fig. 31. Exine exposed to acetolysis followed by potassium permanganate shows a coiled structure in the columella. Bars: 1 μm.

The scanning tunnelling microscopy information from the work of Wittborn *et al.* (1996) on *Fagus* pollen indicates that the subunits are helices about 10-15 nm in width. These subunit helices seemed to be arranged (wrapped) helically into exine units 50-60 nm in width (Wittborn *et al.*, 1998: sketch in Fig. 3C). The subunits appear to be multi-helical with the largest helix 60-80 nm in diameter and with 20-30 nm pitch (Wittborn *et al.*, 1996: Fig. 20). The strands of the helix consist of a smaller helix 20-30 nm in diameter and with a pitch of approximately 9 nm (Wittborn *et al.*, 1996: Fig. 19). These may be seen to some extent in the SEM in Figure 17.

Lilium longiflorum

Some mature *Lilium* pollen was exposed to MMNO·H_2O (Figs. 29, 30) while another sample was exposed to acetolysis followed be potassium permanganate (Fig. 31). Southworth (1985: Figs. 1, 2) showed TEMs of untreated and acetolyzed exines of *L. longiflorum*. The central region of the tectal muri was, in some sections, more subject to erosion by MMNO·H_2O than the surface of the ectexine (Fig. 29), but in other muri there was no such erosion (Fig. 30). The isolated columella in Figure 30 shows an apparently coiled structure, this is a micrograph from the same section as Figure 29. The exine exposed to acetolysis and permanganate also had columellae that showed a coiled structure (Fig. 31).

Lycopodium clavatum

As a result of MMNO·H_2O exposure the exine of *Lycopodium* showed circular and linear structures (Fig. 32). The linear structures are 0.2-0.3 μm in apparent (the boundaries are not sharp) diameter (Figs. 33, 34). The linear structures are marked as between arrowheads in Fig. 33.

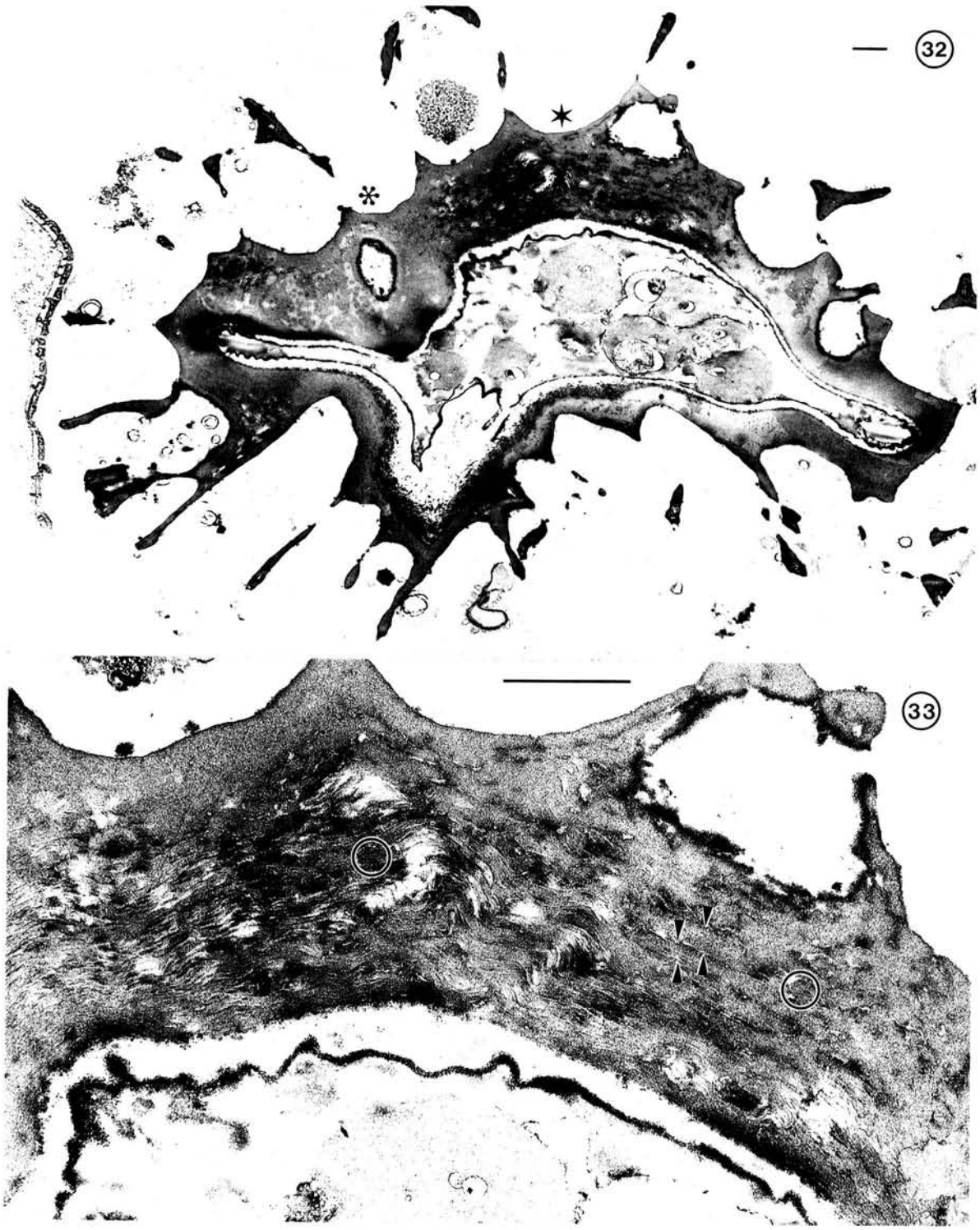

Figs. 32-33. TEMs of *Lycopodium clavatum* exines exposed to $MMNO \cdot H_2O$ for 310 minutes. Fig. 32 is a low magnification micrograph of the entire thin section (the star and asterisk indicate positions of micrographs in Figs. 33 and 34). The exine in these marked regions appears to be thick by virtue of having been sectioned quite obliquely. It is the oblique plane of section that provides information about substructural components in both side and cross-sectional views. Bar: 10 μm. Fig. 33. In some parts of the section the exine appears to be separated or split between closely spaced lamellations. Some of these are interrupted by circular sites (circles). Where lamellations are least distorted there are rod-like parallel (linear) structures (marked at either side by arrowheads). The circled area at the right may enclose an end-view of one of these linear structures. Bar: 1 μm.

Fig. 34. TEM of *Lycopodium clavatum* exine. This part of the obliquely sectioned exine has many of the closely spaced lamellations that show quite distinctly in Fig. 33. In this region many of the linear structures are arranged more-or-less on end and are seen to be circular (two such sites are circled). Bar: 1 μm.

Thin lamellations, about 10 nm wide, were seen following a three-hour exposure to ozone (Rowley, 1995: Fig. 32). Transverse lamellations (Figs. 32-34) were not apparent in mature spores of *Lycopodium* prior to exposure to MMNO·H_2O

According to the AFM results there are radial structural units that appear to be helical in the *Lycopodium* exine. The structural units seem to have radial cross linkages (Fig. 44). In STM, offering better resolution, scans of the *Lycopodium* exine indicate that the units are about 40-60 nm wide and have varying lengths (Fig. 45). Structure of this size and configuration are marked by arrowheads in Figure 33. These units appeared to consist of helical subunits with a diameter of 20-25 nm and a pitch of about 9 nm. These helices may be wrapped in a helical way to make up the units (Fig. 45). In Figure 34 the circular units are seen in end views in many sites. Wittborn *et al.* (1996; 1998) have reported further results on the scans of the *Lycopodium* exine with AFM and STM.

Pinus sylvestris

In immature *Pinus* pollen the alveoli that make up ectexine are all separated by spaces (Figs. 35, 36) that become filled with secondarily accumulated sporopollenin. This accumulation takes place on SAPs; the arrangement of which is very complex in *Pinus* (Figs. 37, 39). In sections of mature pollen exines there can be a contrast distinction between primary accumulated and secondarily accumulated sporopollenin (Fig. 38).

Mature pollen of *Pinus* exposed to MMNO·H_2O shows spinule-like processes at the surface of alveolar walls (Fig. 40). These processes may be related to SAPs exposed on these walls early in development (Figs. 37, 39 and illustrations in Rowley *et al.*, 1999a). There are also exposures of substructural loops (Fig. 41) after MMNO·H_2O. The SAP based cross connections between adjacent alveoli seen in immature stages (Fig. 37) are again apparent in mature exines following MMNO·H_2O (Fig. 42).

DISCUSSION

The method used to decide when to stop the MMNO·H_2O exposure indicated the exines include at least a small amount of polysaccharide. A small number of pollen was washed from the MMNO·H_2O mixture and covered with Toluidine blue. The exposure was stopped after 310 minutes when many exines showed pink-red metachromasia in Toluidine blue. This metachromasia requires that anionic (negative) charges in the specimen be separated by less than 0.4 nm (Pearse, 1961). Most commonly in plant material it is polysaccharides that meet this requirement. Rowley and Prijanto (1977) and Rowley *et al.* (1981a) used this metachromasia to indicate that exines (sporopollenin) were to some extent degraded or eroded. Their interpretation was that the polysaccharide/protein glycocalyx on which the exine formed had been embedded within the sporopollenin exine template much like cellulose encapsulated by accumulation of lignin. When the sporopollenin was eroded by oxidation, glycocalyx components were exposed and can make Toluidine blue metachromatic (pink to red). It would seem unlikely that MMNO·H_2O is directly eroding sporopollenin of the exine. If the pink to red metachromasia is the result of polysaccharides, they may have been leached out of tuft polysaccharide/protein containing cross linkages under the influence of the solvent nature of MMNO·H_2O.

The experiments of Rowley and Prijanto (1977) on selective destruction of the exine resulted in exine remnants that were colourless and nonreactive to both basic dyes and osmium tetroxide. Their remnants were resistant to acetolysis (Erdtman, 1960) but did not take on the yellow to reddish brown colour typical during extended (10-15 minutes) time at 100℃ in the acetolysis mixture or in concentrated sulphuric acid. Rowley and Prijanto (1977) found that remnants retained much of their specific morphology and continued to be autofluorescent in ultraviolet. They concluded that, in so far as those remnants are representative of sporopollenin, sporopollenin is more inert than previously believed; continuing work on stain reactivity of exines is reviewed by Rowley and Rowley (1998). After much less severe treatment than Rowley and Prijanto (1977) it was found that the exines could not only be made unreactive to stains but that condition was easily reversed. Rowley and Rowley (1998) removed the contrastable substance from the exine surface using dilute hydroxide (about 10% NaOH) for a few minutes but freshly boiled distilled water (pH7) for

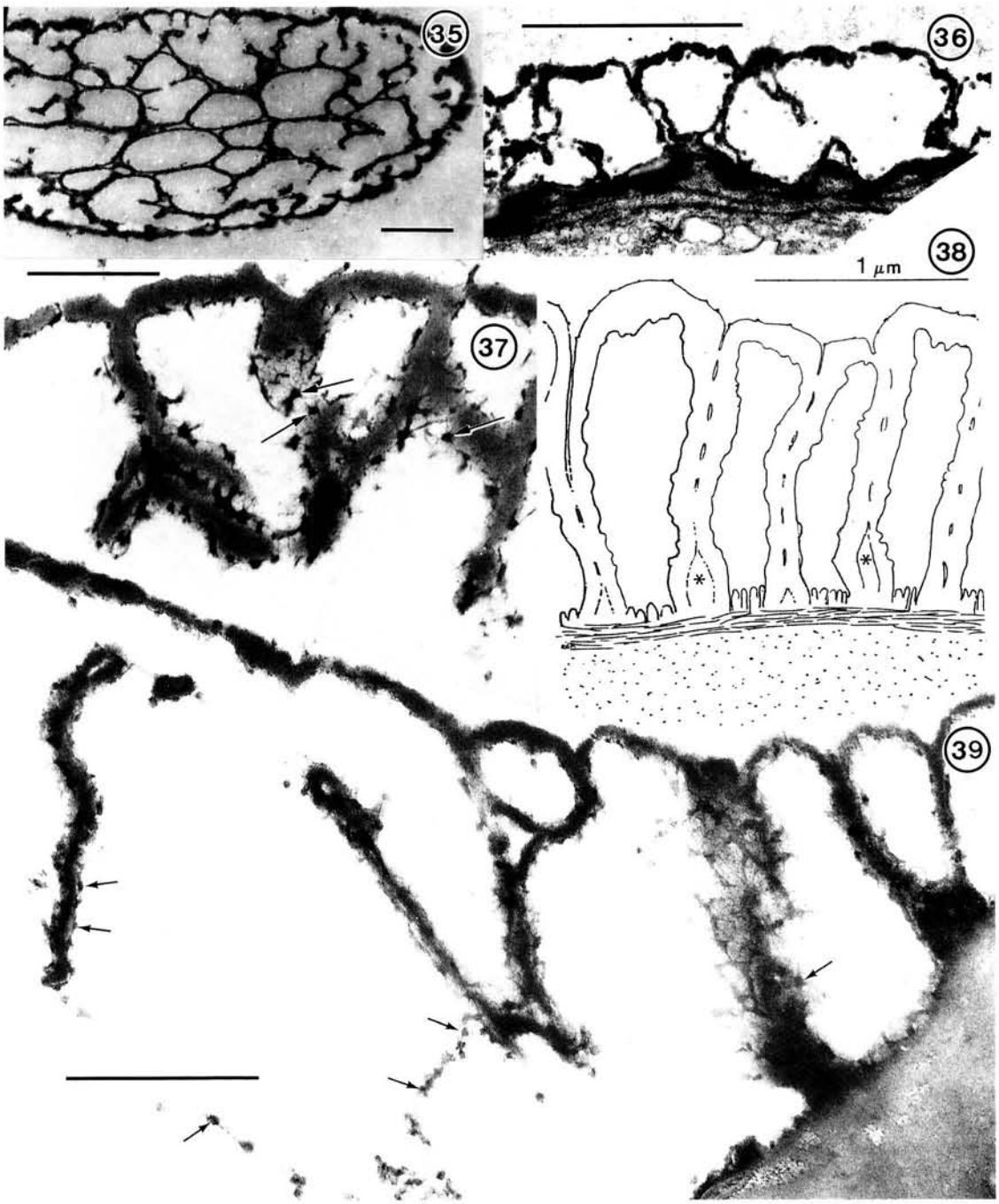

Figs. 35-39. TEMs (Figs. 35-37, 39) of early free microspore stages and sketch (Fig. 38) of mature exine in *Pinus sylvestris*. Bars: 1 μm Figs. 35, 36; Bars: 0.5 μm Figs. 37, 39). Figs. 35, 36. Alveoli are separated from each other. There is a space between each alveolus in sacci (Fig. 35) and in the cap zone (Fig. 36). The space between alveoli is filled by secondarily accumulated sporopollenin on Sporopollenin Acceptor Particles (SAPs, arrows in Fig. 37). There are SAP interconnections between alveolar walls (Fig. 37). Fig. 39. SAPs wrapped around alveolar walls that were separated earlier, as in Figs. 35, 36. Fig. 38. Sketch of alveolar walls in mature pollen. The model is similar to Fig. 36 above except that secondarily accumulated sporopollenin (asterisks) has filled in the spaces between alveoli. In some TEM sections secondarily accumulated sporopollenin can be seen to differ from the primary accumulation of sporopollenin (Rowley, 1990: Fig. 4). Fig. 39. A section emphasizing the inner surfaces of alveoli in a saccus. Complex mature of linked SAPs (arrows) and their very many cross-linkages may be appreciated in this TEM. In some sites SAPs may be seen to be linked as beads on a string (arrows).

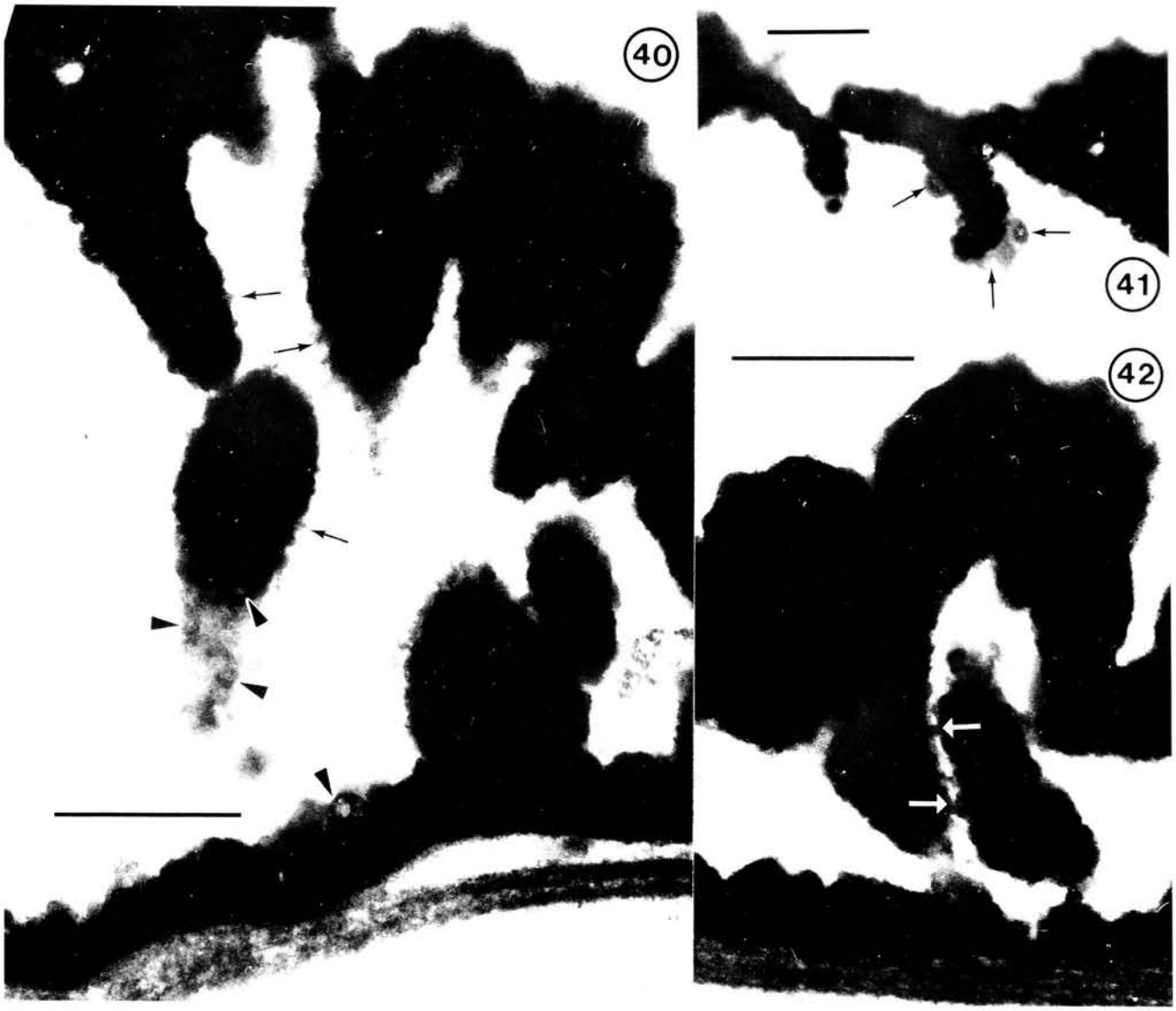

Figs. 40-42. TEMs of mature *Pinus sylvestris* exines exposed to MMNO·H_2O for 310 minutes. The spinule-like processes (arrows) at the surface of the exine in Fig. 40 were not evident in mature pollen before exposure to MMNO·H_2O. These processes are considered to be the SAPs that are seen at earlier stages in development of pollen in *Pinus* (e.g., Rowley *et al.*, 2000: Fig. 13A). Subunit loops are marked by arrowheads. Fig. 41. The micrograph includes several structures, approximately 30 nm wide, that are considered to be loops of the approximately 10 nm diameter subunits (arrows), one of these has a low contrast center. Fig. 42. During exine formation in *Pinus,* all alveoli that make up all of the exines of the taxon are separate and much like nested cups (cf. Figs. 35, 36). The space between alveoli is filled in by secondarily accumulated sporopollenin (see Fig. 37). This filling seems to be removed by exposure to MMNO·H_2O. The cross- links (arrows) in this figure are similar to those in Fig. 37. Bars: 0.5 μm.

30-60 minutes also worked. Exines were made to be reactive again by oxidizing the exine. This could be as mild as 10 minutes on a warm rock in full sunshine, but we used 1% potassium permanganate for 30 seconds. We consider that washing at alkaline pH extracts stainable material from the exine surface while oxidation removes some sporopollenin, exposing stainable material that had been encapsulated within sporopollenin. Several stain reversals brought about by repeated alkaline extraction and oxidation, are illustrated by the

fossil gymnosperm *Classopillis* (Rowley and Srivastava, 1986: Figs. 10, 14-19). The explanation given for this reversal is pertinent to exine erosion by MMNO·H_2O, a potent solvent for polysaccharides (Rowley and Rowley, 1998).

The specific exine morphology of the species forms on surface components of the microspore plasma membrane which we term tufts (Gabarayeva *et al.*, 1998). During exine development, tufts have substructures we refer to as Sporopollenin Acceptor Particles (SAPs), which are like beads (10-15 nm in diameter) on a string at a molecular level (Rowley *et al.*, 1999a). The complexity of the cross-linkages between SAPs may be appreciated to some extent in Figures 37 and 39.

The model for exine substructure in Figure 46 portrays a subunit within a tuft and illustrates our explanation for contrast reversal as well as erosion of exines by a solvent for polysaccharides (MMNO·H_2O). The structure in this model (Fig. 46) with regard to the ten dark spots and their arrangement on the latticework at the bottom of the drawing was worked out and illustrated by Flynn and Rowley (1971). The cross linkages that reach the surface are represented as "star bursts". They are hypothetical but we conceive of them as shown in Figures 37 and 39 (see also Rowley *et al.*, 1999a: Figs. 24-34).

Our idea about exine staining is that after sporopollenin envelopment of the polysaccharide/protein glycocalyx of the plasma membrane surface coating, staining occurs where the glycocalyx side chains reach the exine surface. After extraction of glycocalyx molecules at and near the sporopollenin surface by hydroxide or chlorine, the exine may no longer be stained until after some sporopollenin is etched away, exposing polysaccharide/ protein. It should be noted that Espelie *et al.* (1989) found that there is a carbohydrate domain in sporopollenin based upon ^{13}CNMR spectroscopy. Our interpretation of how it is that exposure to a potent solvent of polysaccharides can bring about erosion of the sporopollenous exine is that MMNO·H_2O first enters the exine through microchannels and then permeates the polysaccharide containing side chains.

An early effect of MMNO·H_2O on the exines was enlargement of microchannels in the *Fagus* exine after only 30 minutes. In *Calluna* such a change in microchannels was the only modification detected in a five-hour exposure. We consider that enlargement of microchannels is not due to etching out or tunnelling out of sporopollenin but simply expanding the exine to the general size of these channels during their active use in transport through the exine. The "expanded" size is seen in the AFM of mature *Betula* pollen (Fig. 43) and in *Triticum* (Fig. 47).

The changes brought about in *Borago* pollen through exposure to MMNO·H_2O actually removed sporopollenin from gemmae. Late in development clumps of SAPs, like those in Figure 12, accumulate sporopollenin. The accumulation results in a specific ornamentation —the gemmae are then covered by many rounded ridges (Fig. 13). We consider that penetration of MMNO·H_2O into the exine occurs by strands of polysaccharide/protein such as those modelled in Figure 46. This results in extraction of the polysaccharide in the mucopolysaccharide of the glycocalyx components embedded in the exine. The remnants of SAPs on the gemmae in Figure 10 contrast positively for protein, but as would be expected, tests for polysaccharide were negative after exposure to MMNO·H_2O. In the early development of *Triticum* microspores (Fig. 48) reported by El-Ghazaly and Jensen (1985, 1986) there are supratectal SAPs like those of *Borago* (Rowley *et al.*, 1999b).

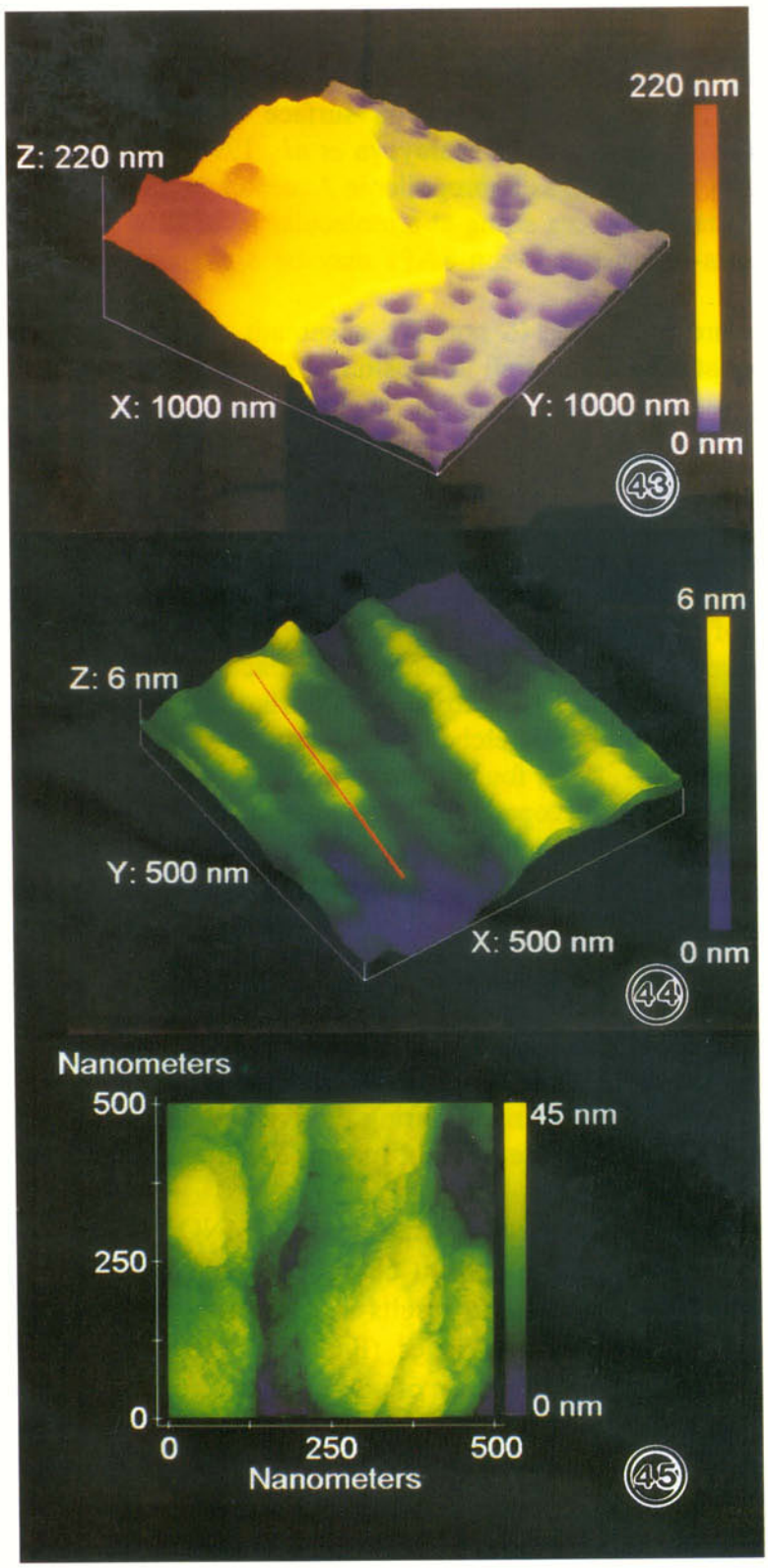

Figs. 43-45. AFM (Figs. 43, 44) and STM (Fig. 45) scans of *Betula pendula* (Fig. 43) and *Lycopodium clavatum* (Figs. 44, 45) exines. Fig. 43. AFM scan showing depressions (channels) in the foot layer of an acetolyzed and freeze sectioned (fractured) exine of *Betula* pollen. The elevated (yellow to red) portion of the 1000 X 1000 nm area scanned is tectum and spinules. Figs. 44. AFM scans of acetolyzed and epoxy embedded spore of *Lycopodium*. The unit structures appear to be helical and to have a longitudinal orientation. In Figs. 33 and 34 circular sites are circled and linear structures are marked by arrowheads. Interpretation of the scans suggested that there are radial cross linkages. The area covered is 500 nm in both the X and Y-axis. The height (Z-axis) is 6 nm; the colour bar shows that the artificial colour is blue for the base through green to yellow for the greatest elevation (6 nm) of the sampled area. The trace for the red line along one of the unit structures indicated that the units have helical subunits and that the subunits consist of smaller components about 10 nm wide. Fig. 45. STM image of an acetolyzed and fractured spore wall of *Lycopodium*. The scan is over an area of 500 X 500 nm. The units are 40-60 nm in width. They appear to consist of helical subunits with diameters of 20-25 nm. These helices may be coiled units.

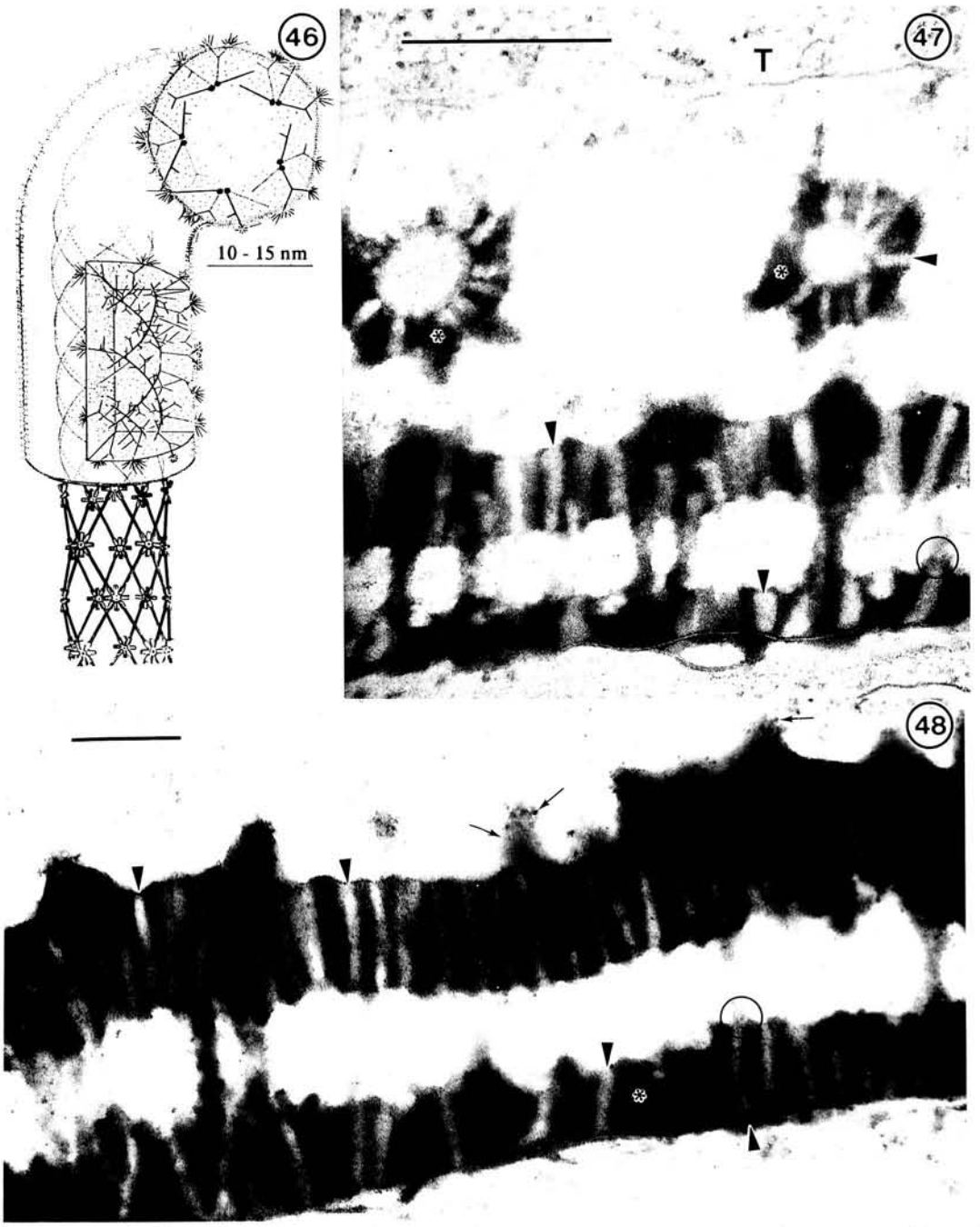

Figs. 46-48. Tuft subunit model (Fig. 46) and TEMs of *Triticum aestivum* (Poaceae; Figs. 47, 48) exines. Fig. 46. Model of tuft subunit given the foghorn shape in an attempt to show substructures face-on as well as in side view. The starburst sites at the surface are to suggest exposed stain-reactive molecules. The pink to red metachromasia in Toluidine blue indicates that such sites are separated by less than 0.4 nm after sporopollenin is etched enough to expose the reactive molecules. The "bare bones" molecular construction at the bottom of the model is intended to depict a plasma membrane surface coating macromolecule without side chains and before accumulation of sporopollenin. Fig. 47. A thin section of a *Triticum* microspore exine and adjacent Ubisch bodies (asterisks) and tapetal cell (T). The microchannels (arrowheads) in the exine and Ubisch bodies are 40-50 nm in diameter, similar to those in the AFM in Fig. 43 and the microchannels after exposure to MMNO·H_2O (e.g., Figs. 3, 16). Strands of "transported" material entering channels are circled. Bar: 0.5 μm. Fig. 48. SAPs (arrows) on forming spinules of a microspore exine. The SAPs are like those of *Borago* (Fig. 12) and *Pinus* (Fig. 39). There are microchannels (arrowheads) in both tectum and foot layer (asterisk). Material entering a channel at time of fixation is circled. Bar: 0.5 μm.

We consider that it is unlikely for sporopollenin to be directly eroded or lost by MMNO·H_2O. MMNO·H_2O actually removes polysaccharides and it is this loss that affects the changes we describe in exine morphology. Following MMNO·H_2O exposure, exines were taken through water and other solvents. Rowley *et al.* (1981a) found that after degradation by acetolysis followed by 2-aminoethanol that the exines were resistant to a second acetolysis, i.e., their morphology was unchanged. They found, however, that these exines fractured into small pieces when washed with water (Rowley *et al.*, 1981b: Figs. 27A, B). The slender portion of *Lilium* columellae is, somewhat like the gemmae of *Borago* with respect to selective erosion by MMNO·H_2O. In this case the coiled substructures of a tuft, the template for columellae, are revealed (Fig. 30). Exposure of acetolyzed pollen of *Lilium* to potassium permanganate also exposes the coils of the tuft basis of columellae of *Lilium* (Fig. 31).

Perhaps a more dramatic effect of MMNO·H_2O on *Lilium* pollen is the erosion of the central part of the massive muri on columellae (Fig. 29). We cannot suggest an explanation for this. The pollen of *L. longiflorum* was donated by Dr. Darlene Southworth and is the same collection used for her study of pollen exine substructure (Southworth, 1985). In her study, after mature pollen was exposed first to acetolysis, then to 2-aminoethanol, there was no indication in the degraded exines or in the untreated controls, of any discontinuities or erosion in the muri (Southworth, 1985).

Rowley *et al.* (1987) found that oxidation of exines with potassium permanganate etched exines of *Betula* at both distal and proximal surfaces and in microchannels. El-Ghazaly and Rowley (1997: Plates 2, 3, 5) showed the untreated and oxidized exines side by side. The material oxidized by permanganate around the microchannels, increasing their size from about 25 nm to 40-50 nm in diameter, would presumably be sporopollenin. Components around microchannels unaffected by oxidation would include carbohydrates and proteins. These components in the 40-50 nm wide "microchannels" were strongly contrasted UA - Pb and appeared to be coiled (Rowley *et al.*, 1987: Pl. 4, 2).

Paxson-Sowders *et al.* (1997) found that sporopollenin in pollen in the wild type of *Arabidopsis thaliana* is accumulated in a regular pattern on the plasma membrane of microspores. But in a mutant the sporopollenin accumulates randomly. Paxson-Sowders *et al.* suggest that sporopollenin formation takes place by self-assembly since, they consider that, sporopollenin on pollen of the mutants accumulates without a stencil. Their "stencil" would be, according to our interpretation, plasma membrane-glycocalyx units (tufts) (e.g., Rowley and Dahl 1982, Rowley *et al.*, 1999b).

There are many experimental results showing that exine not accumulated directly on tufts is less resistant to a variety of oxidative conditions. Some of these have involved using plasma ashing of *Paeonia* pollen (Nowicke *et al.*, 1986); and fast atom etching of *Betula* pollen (Claugher and Rowley, 1987); six years in a biologically active leaf mould (Rowley and Skvarla, 1994; Skvarla *et al.*, 1996), and acetolysis (Erdtman, 1960) followed by oxidation with potassium permanganate on *Quercus coccifera* and *Q. robur* (Rowley and Claugher, 1991). Sporopollenin not accumulated directly in tufts has been referred to as "receptor independent sporopollenin" (Claugher and Rowley, 1990) but currently we use the rather awkward couplet secondarily accumulated sporopollenin. If the idea persists, a single simple word would be useful.

Southworth (1974), in her classical work on exine solubility, determined that the endexine is much more resistant to oxidative conditions than the ectexine. Our MMNO·H_2O results imply that the resistance of the endexine is due to little or no accumulation of secondarily

accumulated sporopollenin. The most important point of this interpretation is that the sporopollenin in the ectexine, accumulated on tufts, is not different from that of the endexine.

Faegri (1936) noted that the endexine in mature pollen exines prepared for LM had less contrast than the ectexine. Faegri's observations have been confirmed by many LM and TEM reports. Rowley (1995) contended that this was due to more rapid or complete extraction of stainable substances than the ectexine. Rowley and Dahl (1977) pointed out that in well-fixed fresh pollen the endexine contrasts much more intensely than the ectexine. Rowley's interpretation is that the solvents commonly used in the preparation of specimens for LM and TEM (especially water) extract contrastable molecules (Rowley, 1995). If this is the case then why is the endexine more porous, absorbent or spongy than the ectexine? In TEM sections the endexine often appears solid and at some stages it is longitudinally traversed by "white lines" that are commonly considered to be lamellations (sheets). If, however, as Rowley (1986, 1987) contends, tufts are plasmodesmatal-equivalents, then transport of supplies when living or extraction during preparation for microscopy is a built-in feature of the endexine. The microchannels in the endexine of *Lopezia lopezioides* (Onagraceae) illustrate how transport can occur (Fig. 49). It would seem that it would be better to call microchannels conduits.

Why are there differences in the erosion in exines of the same species? Rowley *et al* (1981a) found as a result of timed exposures of pollen grains to 2-amino-ethanol that results with respect to exine erosion were reproducible only for pollen at the same level of development, from a single anther and stored under the same conditions (in this experiment, dry acetone). They suggest that reasons for variation in exine resistance could be due to exocellular enzymes, polymerisation level of sporopollenin and/or auto oxidation. Auto oxidation of sporopollenin may be responsible for changes that could occur within seconds (Erdtman, 1943).

ACKNOWLEDGEMENTS

This study was partially supported by a grant from the Russian Foundation of Fundamental Investigations (RFFI) to N. I. Gabarayeva (No. 99-04-49653). Figs. 43-45, the authors thank the Scandinavian University Press and editors of Grana for permission to reproduce micrographs from Wittborn *et al.* (1996); Figs. 1 and 2 are portions of micrographs in Rowley, El-Ghazaly and Rowley; 1987; Fig. 13 is a part of a micrograph in Rowley, Skvarla and Gabarayeva, 1999b; Fig. 16 is a serial section of a micrograph in Dahl and Rowley, 1991; Figs. 35, 37, 39 are from micrographs in Rowley, Skvarla and Walles, 1999a, Figs. 40 and 42 are parts of a micrograph in Rowley, Skvarla and Walles, 2000; Fig. 46 has been modified and redrawn from a sketch from Rowley and Rowley, 1998.

We are most appreciative for the comments and suggestions of the manuscript reviewers.

LITERATURE CITED

Baldi, B. G., V. R. Franceschi and F. A. Loewus. 1987. Preparation and properties of pollen sporoplasts. Protoplasma **141**: 47-55.

Ben Saad-Liman, S. and M. A. Nabli. 1984. Ultrastructure of the exine of *Borago officinalis* (Boraginaceae) pollen. Grana **23**: 1-10.

Claugher, D. and J. R. Rowley. 1987. *Betula* pollen grain substructure revealed by fast atom etching. Pollen et Spores **29**: 5-20.

Claugher, D. and J. R. Rowley. 1990. Pollen exine in *Fagus* (Fagaceae): role of tufts in exine expansion. Can. J. Bot. **68**: 2195-2200.

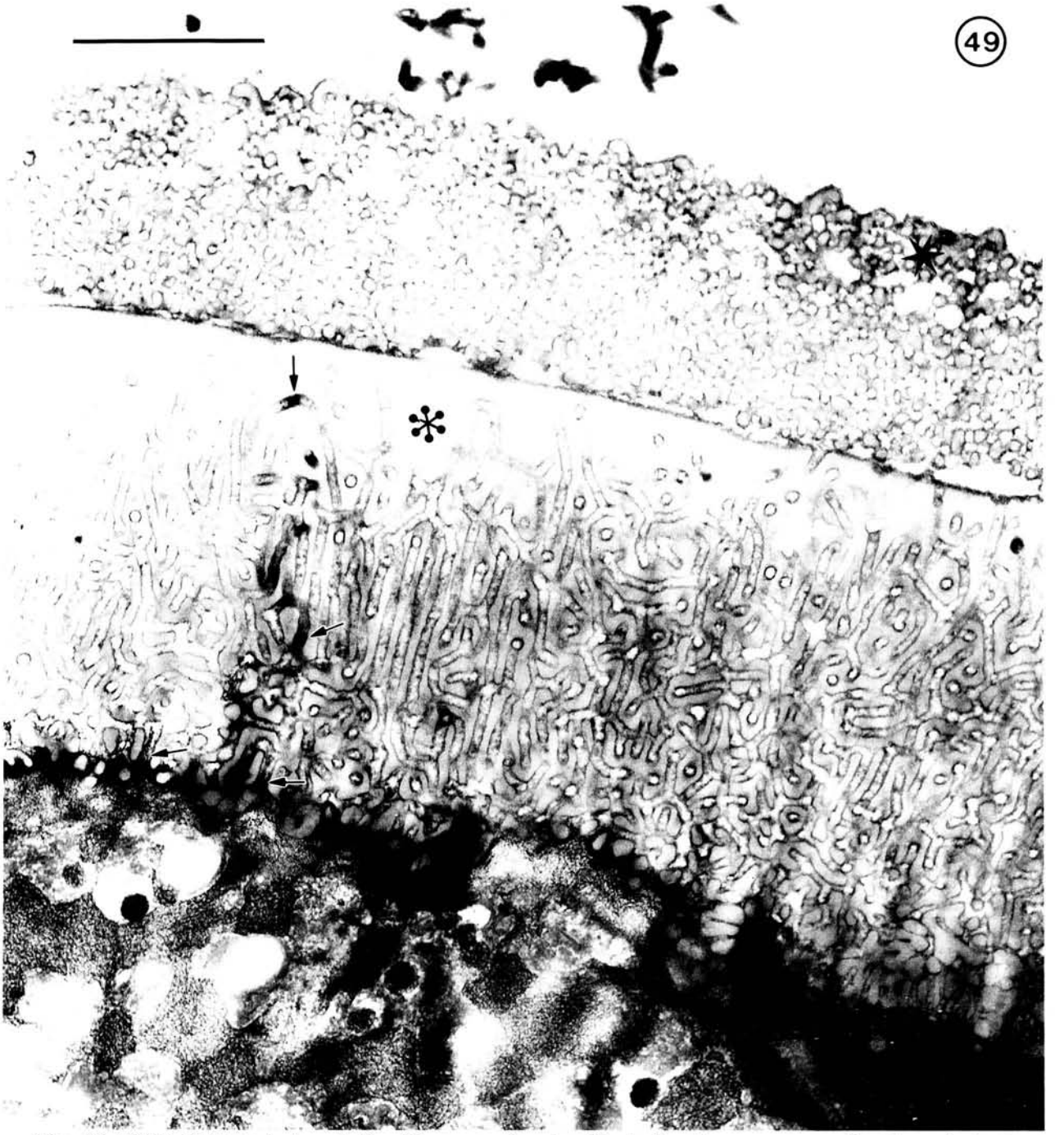

Fig. 49. TEM of *Lopezia lopezioides* (Onagraceae) exine illustrating the numerous microchannels in the endexine. Some channels (arrows) contain darkly contrasted material that was apparently being transported across the endexine (asterisk) into the cytoplasm at the time of fixation for TEM. There is also darkly contrasted material in the ectexine part (star) of the section. Bar: 1 μm.

Dahl, A. O. and J. R. Rowley. 1991. Microspore development in Calluna (Ericaceae). Exine formation. Ann. Sci. Nat. Bot., Paris, 13 serie, **11**: 155-176.

Dunbar, A. and J. R. Rowley. 1984. *Betula* pollen development before and after dormancy: exine and intine. Pollen et Spores **26**: 299-338.

El-Ghazaly, G. and W. A. Jensen. 1986. Studies of the development of wheat (*Triticum aestivum*) pollen: I. Formation of the pollen wall and Ubisch bodies. Grana **25**: 1-29.

El-Ghazaly, G. and W. A. Jensen. 1985. Studies of the development of wheat (*Triticum aestivum*) pollen: III Formation of microchannels in the exine. Pollen et Spores **27**: 5-14.

El-Ghazaly, G. and E. Grafstrom. 1995. Morphological and histochemical differentiation of the pollen wall of *Betula pendula* Roth. during dormancy up to anthesis. Protoplasma **187**: 88-102.

El-Ghazaly, G. and J. R. Rowley. 1997. Pollen wall of *Ephedra foliata*. Palynology **21**: 7-18.

Erdtman, G. 1943. An introduction to pollen analysis. Ronald Press. New York.

Erdtman, G. 1960. The acetolysis method. A revised description. Svensk. Bot. Tidskr. **54**: 561-564.

Erdtman, H. 1943. Chemistry of Peat. In: Erdtman, G. Pollen Analysis. pp. 9-25. Ronald Press. New York.

Espelie, K. E., F. A. Loewus, R. J. Pugmire, W. R. Woolfenden, B. G. Baldi and P. H. Given. 1989. Structural analysis of *Lilium longiflorum* sporopollenin by ^{13}CNMR spectroscopy. Phytochemistry **28**: 751-753.

Faegri, K. 1936. Einige Worte über die Färbung der für die Pollenanalyse hergestellten Präparate. Geol. för Stockholm förhdl. **58**: 439-443.

Faegri, K. and J. Iversen. 1989. Textbook of pollen analysis. 4th ed. (By K. Faegri, P. E. Kalland and K. Krzywinski). J. Wiley and Sons, Chichester-New York-Brisbane-Toronto -Singapore.

Faegri, K. and L. Van Der Pilj. 1966. The principles of pollination ecology. Pergamon Press. Oxford.

Flynn, J. J. and J. R. Rowley. 1971. Wall microtubules in pollen. Zeiss Informationen **76**: 40-45.

Gabarayeva, N. I., J. R. Rowley and J. J. Skvarla. 1998. Exine development in *Borago* (Boraginaceae). 1. Microspore tetrad period. Taiwania **43**: 203-214.

Hesse, M. 1985. Hemispheric surface processes of exine and orbicules in *Calluna* (Ericaceae). Grana **24**: 93-98.

Loewus, F. A., B. G. Baldi, V. R. Franceschi, L. D. Meinert and J. J. McCollum. 1985. Pollen sporoplasts: dissolution of pollen walls. Plant Physiol. **78**: 652-654.

Moore, P. D., J. A. Webb and M. E. Collinson. 1991. Pollen analysis. Blackwell Sci. Publ., Oxford.

Mollenhauer, H. H. 1964. Plastic embedding mixtures for use in electron microscopy. Stain Technol. **39**: 111-115.

Nowicke, J. N., J. L. Bittner and J. J. Skvarla. 1986. *Paeonia* exine and plasma etching. In: Blackmore, S. and I. K. Ferguson (eds.). Pollen and Spores. Form and Function. Linnean Society Symposium. Ser. 12 (pages 81-95). Academic Press, London.

Paxson-Sowders, D. M., H. A. Owen and C A. Makaroff. 1997. A comparative ultrastructure analysis of exine pattern development in wild-type *Arabidopsis* and a mutant defective in pattern formation. Protoplasma **198**: 53-65.

Pearse, A. E. G. 1961. Histochemistry. Little, Brown & Co., Boston.

Pease, D. C. 1968. Phosphotungstic acid as an electron stain. 26th Ann. Proc. Electron Micro. Soc. America: pp.36-37. Clatior's, Baton Rouge.

Rowley, J. R. 1986. A model for plasmodesmata. pp. 175-180. In: Cresti, M. and R. Dallai (eds.) Biology of reproduction and cell motility in plants and animals. University of Siena - Italy.

Rowley, J. R. 1987. Plasmodesmata-like processes of tapetal cells. La Cellule **74**: 229-241.

Rowley, J. R. 1995. Are endexines of pteridophytes, gymnosperms and angiosperms

structurally equivalent? Rev. Paleobot. Palynol. **85**: 13-34.
Rowley, J. R. 2001. Why the endexine and ectexine differ in resistance to oxidation. *Calluna* as a model system. Grana **40**: 165-169.
Rowley, J. R. and A. O. Dahl. 1977. Pollen development in *Artemisia vulgaris* with special reference to glycocalyx material. Pollen et Spores **19**: 169-284.
Rowley, J. R. and A. O. Dahl. 1982. A similar substructure for tapetal surface and exine "tuft" units. Pollen et Spores **24**: 5-8.
Rowley, J. R. and S. K. Srivastava. 1986. Fine structure of *Classopollis* exines. Can. J. Bot. **64**: 3059-3074.
Rowley, J. R. and J. S. Rowley. 1998. Stain reversal on pollen exines. In; Current Concepts in Pollen-Spore and Biopollution Research (N. M. Dutta, S. Gupta-Bhattacharya, S. Mandal and K. Bhattacharya, eds.). Pp. 223-232. Research Periodicals & Book Publishing House. USA-UK-India-Taiwan.
Rowley, J. R., A. O. Dahl, S. Sengupta and J. S. Rowley. 1981a. A model of exine substructure based on dissection of pollen and spore exines. Palynology **5**: 107-152.
Rowley, J. R., A. O. Dahl and J. S. Rowley. 1981b. Substructure in exines of Artemisia vulgaris (Asteraceae). Review of Palaeobotany and Palynology **35**: 1-38.
Rowley, J. R., G. El-Ghazaly and J. S. Rowley. 1987. Microchannels in the pollen grain exine. Palynology **11**: 1-21.
Rowley, J. R. and D. Claugher. 1991. Receptor-independent sporopollenin. Bot. Acta **104**: 316-323.
Rowley, J. R. and B. Prijanto. 1977. Selective destruction of the exine of pollen grains. Geophytology *7*: 1-23.
Rowley, J. R. and J. J. Skvarla. 1994. Corroded exines from Havinga's leaf mold experiment —Structure of *Fagus* and *Quercus* exines. Rev. Palaeobot. Palynol. **83**: 65-72.
Rowley, J. R., J. J. Skvarla and B. Walles. 1999a. Microsporogenesis in *Pinus sylvestris* –VII. Exine expansion and tapetal development. Taiwania **44**: 325-344.
Rowley, J. R., J. J. Skvarla and N. I. Gabarayeva. 1999b. Exine development in *Borago* (Boraginaceae). 2. Free Microspore Stages. Taiwania **44**: 212-229.
Skvarla, J. J., J. R. Rowley and W. F. Chissoe. 1996. Corroded exines from Havinga's leaf mold experiment. SEM. Palynology **20**: 191-207.
Southworth, D. 1974. Solubility of pollen exines. Amer. J. Bot. **61**: 36-44.
Southworth, D. 1985. Pollen exine substructure. I. *Lilium longiflorum*. Amer. J. Bot. **72**: 1274-1283.
Tarlyn, N. M., V. R. Franceschi, J. D. Everard and F. Loewus. 1993. Recovery of exines from mature pollens and spores. Plant Sci. **90**:219-224.
Thom, I., M. Grote, J. Abraham-Peskir and R. Wiermann. 1998. Electron and X-ray microscopic analyses of reaggregated materials obtained after fractionation of dissolved sporopollenin. Protoplasma **204**: 13-21.
Wittborn, J., K. V. Rao, G. El-Ghazaly and J. R. Rowley. 1996. Substructure of spore and pollen grain exines in *Lycopodium*, *Alnus*, *Betula*, *Fagus* and *Rhododendron*. Investigation with Atomic Force and scanning tunnelling microscopy. Grana **35**: 185-196.
Wittborn, J., K. V. Rao, G. El-Ghazaly and J. R. Rowley. 1998. Nanoscale similarities in the substructure of exines of the exines of *Fagus* pollen grains and *Lycopodium* spores. Annals Bot. **82**: 141-145.

MMNO·H_2O 在花粉和孢子外壁產生的效應

John R. Rowley[1, 5], Nina I. Gabarayeva[2], John J. Skvarla[3] and Gamal El-Ghazaly[4]

(收稿日期：2001 年 8 月 2 日；接受日期：2001 年 9 月 6 日)

摘　　要

將垂枝樺、玻璃苣、加蘆那杜鵑、歐洲水青岡、麝香百合和歐洲赤松的成熟花粉粒及石松的孢子暴露在 80°C 的 MMNO·H_2O 下，處理時間由 30 分鐘至 310 分鐘。30 分鐘後小通道的直徑大約從 25 nm 擴張為 50 nm，一般通道的大小在發育期間大概是 50 nm。除加蘆那杜鵑外，觀察其他種類花粉在處理近五個小時後的變化。玻璃苣和歐洲赤松在花粉外壁形態上所產生的變化，與我們先前研究中所指出在外壁發育晚期才添加的孢粉質有關。花粉外壁發育的早期，孢粉質堆積在部份細胞膜表面的覆蓋物上(即網叢，外壁單元結構)，也就是孢粉質接受粒上。在外壁發育的晚期，次級孢粉質堆積於網叢之間或是它們的表面。這個階段中，孢粉質接受粒會交叉連結遍及整個外壁上。我們的推測是 MMNO·H_2O 對於多醣類就像是一種有效的溶劑，可經由網叢內的小通道和網叢交叉連結之間滲入外壁中。一般的穿透式電子顯微鏡樣品製作過程中，由於花粉暴露在水和溶劑中使多醣類被移除，而引起外壁組成產生裂縫。垂枝樺和歐洲水青岡的花粉在 MMNO·H_2O 中所產生的外壁變化，同樣被推測可能因為溶劑的侵蝕是平行於網叢核心和它的次級結構單位。麝香百合花粉外壁上大多數較細長的柱狀體明顯是由一個網叢所形成，被侵蝕後露出外層的纏繞物。石松孢子經處理後所顯露的是較緊密的間隔，大約是 10 nm，周圍則呈薄層狀排列，且聚集為線狀結構。這些線狀結構在橫切面中觀察為環狀，直徑變化較大(約 100-200 nm)。使用原子力和隧道式掃描電子顯微鏡進行觀察後，推測大部分長的次級單位呈螺旋狀。同樣地，可以觀察到在結構間是放射狀交叉連結的型式。相較下，花粉外壁沒有產生變化的種類，可能必須近一步觀察這些花粉的外壁內層。我們的推測是：花粉外壁內層因為網叢填塞緊密，也沒有一些孢粉素的次級堆積，因而較外壁外層具有較大的抗性。

關鍵詞：原子力顯微鏡，樺木屬，玻璃苣屬，加蘆那杜鵑屬，花粉外壁外層，花粉外壁內層，水青岡屬，百合屬，*Lopezia*，石松屬，小通道，MMNO·H_2O，松屬，孢粉質次級堆積，孢粉質接受粒，隧道式掃描電子顯微鏡，小麥屬，網叢。

1. 斯德哥爾摩大學，植物學系，斯德哥爾摩 SE-106 91，瑞典。
2. 科曼洛夫植物研究所，Popov st. 2，聖彼得堡，197376，俄羅斯。
3. 奧克拉荷馬大學，植物—微生物學系，奧克拉荷馬生物調查部，Norman，OK 73019-6131，美國。
4. 我們的合作者，於 2001 年 1 月 13 日過世。
5. 通信作者。